Journal of Applied Electrochemistry (2005) 35:955–965
DOI 10.1007/s10800-005-7173-4

The electro-reduction of carbon dioxide in a continuous reactor

HUI LI and COLIN OLOMAN*
Department of Chemical and Biological Engineering, University of British Columbia, Vancouver B.C., V6T 1Z4 Canada
*(*author for correspondence, fax: +604-266-1075; e-mail: coloman@intergate.ca)*

Received 19 September 2004; accepted in revised form 13 April 2005

Key words: carbon dioxide, continuous reactor, electro-reduction, formate, tinned-copper mesh

Abstract

This paper reports an investigation into the electro-reduction of CO_2 in a laboratory bench-scale continuous reactor with co-current flow of reactant gas and catholyte liquid through a flow-by 3D cathode of 30# mesh tinned-copper. Factorial and parametric experiments were carried out in this apparatus with the variables: current (1–8 A), gas phase CO_2 concentration (16–100 vol%) and operating time (10–180 min), using a cathode feed of [CO_2 + N_2] gas and 0.45 M $KHCO_3$(aq) with an anolyte feed of 1 M KOH(aq), in operation near ambient conditions (ca. 115 kPa(abs), 300 K). The primary and secondary reactions here were respectively the reduction of CO_2 to formate ($HCOO^-$) and of water to hydrogen, while up to ca. 5% of the current went to production of CO, CH_4 and C_2H_4. The current efficiency for formate depended on the current density and CO_2 pressure, coupled with the hydrogen over-potential plus mass transfer capacity of the cathode, and decreased with operating time, as tin was lost from the cathode surface. For superficial current densities ranging from 0.22 to 1.78 kA m^{-2}, the measured values of the performance indicators are: current efficiency for $HCOO^-$ = 86–13%, reactor voltage = 3–6 Volt, specific energy for $HCOO^-$ = 300–1300 kWh kmol^{-1}, space-time yield of $HCOO^-$ = 2×10^{-4}–6×10^{-4} kmol m^{-3} s^{-1}, conversion of CO_2 = 20–80% and yield of organic products from CO_2 = 6–17%.

Nomenclature

a	specific surface area of cathode, m^{-1}
a_k	Tafel constant for reaction k, V
a_{2Cu}	Tafel constant for reaction 2 on copper, V
a_{2Sn}	Tafel constant for reaction 2 on tin, V
CD	current density, kA m^{-2}
CE_k	current efficiency for reaction k, –
D	diffusion coefficient of CO_2(aq), m^2 s^{-1}
d	wire diameter in cathode mesh, m
d_b	bubble diameter, m
E	electrode potential, V(SHE)
E_{cell}	full-cell operating voltage (absolute value), V
$E_{r,k}$	reversible electrode potential of reaction k, V(SHE)
E°_k	standard electrode potential of reaction k, V(SHE)
ΔE	voltage window in operation of 3D flow-by electrode, V
F	Faraday's number, kC kmol^{-1}
G	gas load in 3D flow-by electrode, kg m^{-2} s^{-1}
h	liquid hold-up in 3D flow-by electrode, –
I	current, kA
i	superficial current density, kA m^{-2}
i_{iL}	mass transfer limited superficial current density for reaction 1, kA m^{-2}
j_k	partial real current density of reaction k, kA m^{-2}
j_{1L}	mass transfer limited real current density for reaction 1, kA m^{-2}
K', K_0, K_1	reaction equilibrium constants, –, M kPa^{-1}, M
k_F	mass transfer coefficient due to forced convection, m s^{-1}
k_G	mass transfer coefficient due to gas (H_2) generation, m s^{-1}
k_M	combined mass transfer coefficient, m s^{-1}
L	liquid load in 3D flow-by electrode, kg m^{-2} s^{-1}
P	total pressure, kPa(abs)
p_{CO_2}	partial pressure of CO_2, kPa(abs)
p_{H_2}	partial pressure of H_2, kPa(abs)
R	gas constant, kJ kmol^{-1} K^{-1}
Re_b	Reynolds' number for bubble generation at electrode, –
Re_g	Reynolds' number for gas flow = $v_g d\,\rho_g/\mu_g$, –
Re_l	Reynolds' number for liquid flow = $v_l d\,\rho_l/\mu_l$, –
SE	specific energy for formate production, kWh kmol^{-1}

Sc	Schmidt number $= \mu_l/\rho_l D$, –
STY	space-time-yield, kmol m^{-3} s^{-1}
T	temperature, K
t	operating time, min
v_g, v_l	superficial gas velocity, superficial liquid velocity, m s^{-1}
X_1, X_2, X_3	factorial variables defined in Table 2, A, min, vol%
x	conversion of CO_2, –
y	volume fraction (i.e. mole fraction) in gas phase, –
ε	porosity of 3D flow-by electrode, –
η_k	over-potential of reaction k, V
θ	coverage of cathode surface by tin, –
γ	activity coefficient, –
κ	conductivity of electrolyte, S m^{-1}
κ_e	effective conductivity of electrolyte, S m^{-1}
μ_l, μ_g	viscosity of liquid, viscosity of gas, kg m^{-1} s^{-1}
ρ_l, ρ_g	density of liquid, density of gas, kg m^{-3}
τ	thickness of 3D flow-by electrode, m
τ_{eff}	effective electro-active thickness of 3D flow-by electrode, m

1. Introduction

Carbon dioxide is now widely accepted as a main contributor to global warming and there is a looming need for methods to sequester this greenhouse-gas and/or to convert it to useful products. Electrochemical processing is seen in this context as a candidate method to convert CO_2 to organic compounds such as the acids, alcohols and hydrocarbons of low molar mass [1].

The latest review [2] and its associated sources show that the electro-reduction of CO_2 has been studied since the late nineteenth century and is known to give a range of products, such as those indicated in Table 1. The majority of this previous work has focused on the electro-catalysis and mechanistic aspects of CO_2 reduction, with experiments carried out in the batch mode in small (e.g. 1×10^{-4} m^2) electrochemical cells (or half-cells) under conditions that are unlikely to sustain a practical process.

The electro-reduction of carbon dioxide in aqueous solution to formate (or formic acid) has had special attention in the literature due to the useful selectivity for this reaction on cathode materials of high hydrogen over-potential (i.e. low exchange current density for hydrogen evolution), such as indium, lead, mercury and tin [3–7]. The exchange current densities for CO_2 reduction to formate at 293 K (in 0.95 M KCl + 0.05 M $NaHCO_3$) on In, Hg and Sn are reported respectively as: 1×10^{-7}, 5×10^{-10} and 1×10^{-8} kA m^{-2} [8], with the primary electro-active species in the cathode reaction being CO_2(aq), engaged in a multi-step adsorption/reaction process involving the intermediate radical anion $CO^{\cdot -}_{2\ ads}$ which is sequentially hydrolyzed and reduced to $HCOO^-$ [2, 3, 8, 9]. Little information is available on the effect of temperature on the reaction kinetics. In this respect one study shows that over the range 293–373 K, the current efficiency for formate decreases with temperature on both In and Sn cathodes, but on Pb goes through a maximum near 333 K [6]. Another study reports the apparent activation energy for the electro-reduction of CO_2 on copper (to unstated products) over the range 298–358 K as 100×10^3–70×10^3 kJ $kmol^{-1}$ [9].

Table 1. CO_2 electro-reduction reactions [2]

Reaction	E^o/V(NHE) 298 K
$2CO_2 + 2H^+ + 2e^- \rightarrow H_2C_2O_4$	−0.475
$CO_2 + 2H^+ + 2e^- \rightarrow HCOOH$	−0.199
$CO_2 + 2H^+ + 2e^- \rightarrow CO + H_2O$	−0.109
$CO_2 + 4H^+ + 4e^- \rightarrow HCHO + H_2O$	−0.071
$CO_2 + 6H^+ + 6e^- \rightarrow CH_3OH + H_2O$	+0.030
$CO_2 + 8H^+ + 8e^- \rightarrow CH_4 + 2H_2O$	+0.169

The relatively low solubility of CO_2 in aqueous solutions (ca. 70 mM at STP), coupled with the $CO_2(aq)/HCO_3^-/CO_3^{2-}$ equilibria, creates a mass transfer constraint on the reaction that limits the primary (steady-state) current density to a maximum value of the order 0.1 kA m^{-2} (i.e. 10 mA cm^{-2}) under the typical laboratory reaction conditions, with 100 kPa(abs) CO_2 pressure at 298 K [2–8, 9]. The intrinsic reaction order with respect to the CO_2 pressure is 0.6–1.0 (depending on the cathode material and potential) with partial current densities ranging up to 1.6 kA m^{-2} (i.e. 160 mA cm^{-2}) recorded under 3000 kPa(abs) CO_2 pressure at a cathode potential of ca. −1.5 V(SHE) [5, 8, 9]. De-activation of the cathode over time (e.g. 1 h) has been observed for CO_2 reduction on copper electrodes [2, 3], and some effects of this type have been indicated on lead and tin [7, 8].

Of the few reported full-cell experiments on the electro-reduction of CO_2 those of Udupa et al. [10] give a current efficiency for CO_2 reduction to formate of ca. 80% at 0.2 kA m^{-2} (i.e. 20 mA cm^{-2}) on a rotating amalgamated (mercury) copper cathode, in a CO_2 gas sparged diaphragm cell with an operating (full-cell) voltage of 3.5 Volt and cathode potential about −1.7 V(NHE). These authors also state that replacing the diaphragm separator by a cation-exchange membrane allowed formate to accumulate to a concentration of ca. 2.8 M in their batch cell, while the current efficiency was maintained around 80%.

Several devices have been suggested to relieve the CO_2 mass transfer constraint noted above. Such devices include operation at super-atmospheric pressure and/or sub-ambient temperature, using a gas-diffusion cathode (GDE) or using a fixed-bed cathode while providing a "3-phase interface" for the reaction by sparging the cathode

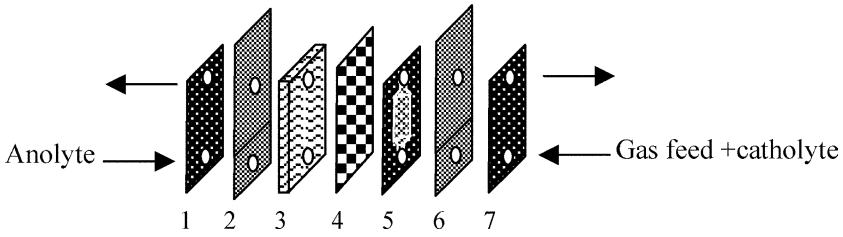

Fig. 1. Cell configuration. 1 and 7: gaskets; 2: anode (platinized titanium); 3: anode spacer (polypropylene mesh); 4: membrane; 5: tinned-copper mesh; 6: cathode feeder (tinned-copper sheet). Compression plates and bolts are not shown.

chamber with CO_2 gas. For example, Hara and Skata [11] reported a total current efficiency of 50% (5 products) at 6 kA m^{-2} on a Pt GDE under 2000 kPa(abs) CO_2 pressure, while Yano et al. [12] obtained 72% total current efficiency (10 products) at 0.1 kA m^{-2} using a copper mesh cathode sparged by CO_2 gas at ca. 100 kPa(abs). In a recent article, Akahori et al. [13] describe a continuous flow-by reactor in which CO_2 in solution (i.e. single-phase flow) is electrochemically reduced to formate on a glass fiber reinforced lead "wire" bundle cathode with almost 100% current efficiency at an apparent current density about 0.02 kA m^{-2} and a full-cell voltage of 1.4 V, obtained by using a Nafion 117 separator and depolarizing the anode with SO_2.

From this summary it is evident that, should it ever be needed, the scale-up of the electro-reduction of CO_2 to attack the greenhouse-gas problem will be a substantial engineering challenge. The work described below is a result of our ongoing investigation into the use of co-current two-phase (G/L) flow in a fixed-bed flow-by electrode [14, 15] of a continuous reactor for the electro-reduction of CO_2 in aqueous electrolytes.

2. Experimental methods

Figure 1 shows the configuration of the single-cell flow-by electrochemical reactor used in this work. The reactor consisted of a tinned-copper feeder plate and tinned-copper mesh cathode, a Nafion 450 cation-exchange membrane separator, polypropylene mesh anode spacer/membrane support, a platinized titanium anode plate and neoprene gaskets. The active cathode dimensions were: length (i.e. height) 150 mm, width 30 mm and thickness ca. 0.6 mm, in which the 3D cathode consisted of a $30^{\#}$ mesh metal screen (ARGUS Corp USA) with 0.3 mm wire diameter, 41% open space and a specific surface of about 7000 m^{-1}. The active anode area matched the superficial area of the cathode, with a $10^{\#}$ mesh anode spacer thickness of 3 mm.

In the plating procedure for the tinned cathode [16], the copper substrate (mesh or feeder plate) was first etched in 7 wt% nitric acid and washed in distilled water, then immersed for 3 min at 319 K in an electroless acidic tin plating bath consisting of 0.02 M stannous sulphate ($SnSO_4$) and 0.22 M sulfuric acid in water with 0.6 M thiourea as the reductant. The cathode mesh, the anode spacer and the membrane were sealed on their margins by silicone glue, then the cell assembly was sandwiched between insulated mild steel plates and uniformly compressed with 8, 1/4 inch bolts (not shown) to give a balanced fluid distribution.

The process flow diagram is shown in Figure 2. In this system, pure CO_2 or a mixture of CO_2 and N_2 gas was combined with the catholyte of 0.45 M $KHCO_3$ and entered the cathode chamber from the bottom to give co-current upward 2-phase (G/L) flow. The anolyte, of 1 M KOH, passed upward through the anode chamber. The fluids were fed through individual rotameters, and their flow rates manually controlled to obtain the appropriate gas and liquid loads for pulsing G/L flow in the cathode [15]. The reactor inlet and outlet pressures and temperatures were measured by visual gauges at the points indicated in the flowsheet. In some runs, the catholyte product temperature was controlled by pre-cooling the anolyte feed to about 290 K.

The cathode gas product was analyzed for CO_2 and CO with an Orsat, and also sampled into a Tedlar bag

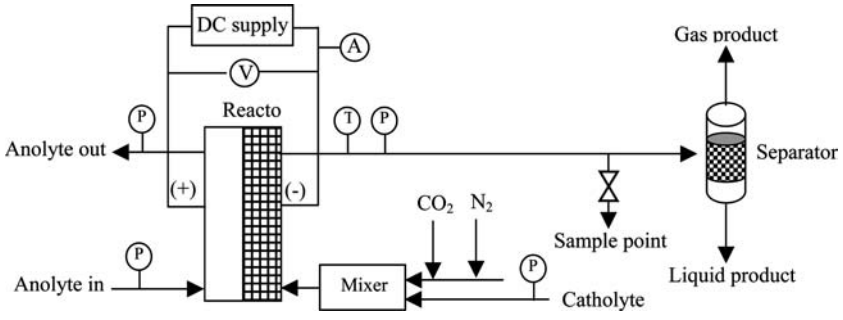

Fig. 2. Process flow diagram. A = ammeter, P = pressure gauge, T = thermometer, V = Voltmeter.

for subsequent determination of hydrocarbons by gas chromatograph (Varian 3600) with an FID detector and Carboxen-1010 PLOT capillary column. The hydrogen content of the product gas (dry basis) was found as the difference between 100% and the sum of the CO_2, CO, CH_4 and C_2H_4 values. In the analysis of the cathodic liquid products, formate was determined by the alkaline permanganate oxidation technique [17] and methanol/formaldehyde was estimated by back-titration with ferrous ammonium sulphate of the product from acid dichromate oxidation. To establish the carbon balance the feed and product carbonate/bicarbonate concentrations at the cathode side were determined by the sequential titration of the catholyte samples with hydrochloric acid, using phenolphthalein and methyl orange as indicators [17]. The anolyte liquid feed and product hydroxide content were determined by titration with hydrochloric acid and phenolphthalein indicator.

Galvanostatic experiments were carried out with a DC power supply, using a separate voltmeter to measure the full-cell operating voltage (i.e. including the anode potential, cathode potential and Ohmic voltage drop).

3. Experimental design

As in any electrochemical system involving multiple reactions with mass transfer constraints, the performance of a reactor for electro-reduction of CO_2 depends on the effects and interactions of many variables, including: the electrode material, reactor configuration and size, anolyte and catholyte composition, CO_2 pressure, temperature, fluid flow rates (more correctly the gas and liquid loads), current density, separator properties and the operating time [18]. Although there are many publications on the electro-reduction of CO_2, these sources cover a huge array of conditions and present a disjointed picture from which it is very difficult to find comprehensive data on which to base a practical process design. Our approach to resolving this problem is to carry out a set of factorial and parametric experiments to systematically explore the effects of some major variables in the bench-scale continuous reactor described above.

This paper presents the results of experiments with the three variables: current, operating time (i.e. cathode age) and CO_2 concentration in the feed gas, first in the 2^3 factorial design outlined in Table 2 and then in parametric experiments that examine the effect of each of these variables while the others are held constant. In all of these runs, other conditions expected to affect the process were kept constant or in the ranges shown in Table 3.

4. Results and discussion

4.1 *Factorial experiments*

The factorial runs were carried out in random order with three replicates of the center-point. Replicates were also made for two corner-points and these data were pooled to calculate the confidence level of the results.

Including center-points and replicates, 16 experimental runs were carried out in this factorial set. In all of these runs, formate and hydrogen were the dominant

Table 2. Factorial variables and levels

Variable	Symbol	Units	Level		
			High	Low	Center
			+	−	0
Current	X_1	A	6	2	4
Operating time	X_2	min	30	10	20
CO_2(g) feed concentration	X_3	vol%	100	33	67

Table 3. Other process conditions

Condition	Units	Value
Reactor configuration and size	–	As described above
Cathode bed material	–	1 layer, 30# mesh tinned-copper
Cathode feeder material	–	Tinned-copper plate
Total pressure in cathode	kPa(abs)	102–160
Total pressure in anode	kPa(abs)	104–160
Catholyte temperature	K	296–303
Catholyte feed composition	–	0.45 M $KHCO_3$
Anolyte temperature	K	290–303
Anolyte feed composition	–	1.0 M KOH
Anolyte feed flow	$m^3\ s^{-1}$	5.0×10^{-7} (i.e. 30 ml min^{-1})
Catholyte feed flow	$m^3\ s^{-1}$	3.3×10^{-7} (i.e. 20 ml min^{-1})
Cathode gas feed flow	$m^3\ s^{-1}$ STP	3.0×10^{-6} (i.e. 180 ml min^{-1} STP)
Catholyte pH	–	7–8

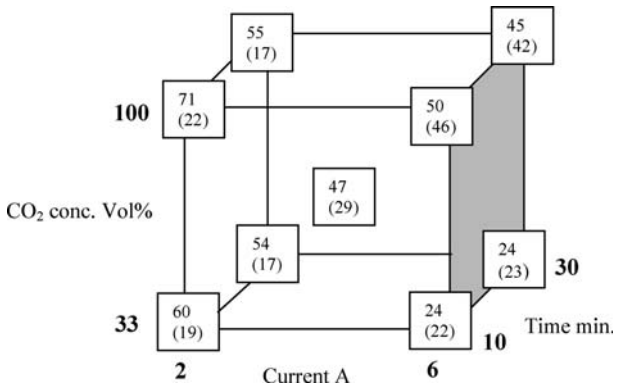

Fig. 3. Factorial results for $HCOO^-$ production. [CE for $HCOO^-$%, ([$HCOO^-$] mM)].

cathode products, accounting for 95–99% of the current. Methane and ethylene were detected but negligible (< 0.06 vol%) and the current efficiency for carbon monoxide ranged from 0 to 5%. A crude analysis of the catholyte product by dichromate oxidation indicated that up to about 5% of the CO_2 reduction products in the liquid phase were compounds other than formate (e.g. formaldehyde and methanol) but a complete accounting for these tertiary products was not attempted.

The principal results of these runs with respect to formate production are shown in the factorial cube of Figure 3. A check on the integrity of these data is provided by the cathode current efficiency and overall carbon balances summarized in Table 4.

The analysis of variance summarized in Table 5 shows significant effects (at the 95% confidence level) on the formate CE for each of the main factors (X_1, X_2 and X_3) plus the (X_1X_3) interaction, with an insignificant curvature over the experimental space [19].

4.1.1. *Main and interaction effects*

Table 5 shows that current has the strongest main effect on both the formate CE and [$HCOO^-$], but in opposite directions, i.e. the effect of increasing the current from 2 to 6 A, averaged over all levels of CO_2 feed concentration and cathode age, is to lower the CE by 24% while raising the $HCOO^-$ product concentration by 15 mM.

The main effects of cathode age on both the CE and [$HCOO^-$], respectively −6.9% and −2.7 mM, indicate deactivation of the cathode. The "poisoning" of copper cathodes for CO_2 reduction has been widely reported [2, 3] and deactivation of tin cathodes has also been observed [7, 8]. In the present work, the SEM images and EDX spectra of new and used cathodes in Figure 7 show a progressive loss of tin from the cathode surface that probably accounts for the effect of cathode age.

The positive effect of CO_2(g) concentration in the gas feed on both CE and [$HCOO^-$] (14.6% and 11.6 mM, respectively) reflects the fact that CO_2(aq) is the electroactive species and an increase in its level promotes both the intrinsic kinetic and mass transfer processes of the primary cathode reaction. This effect is reinforced in the positive (X_1X_3) interaction which shows that a higher current (i.e. current density) is supported by an increased CO_2 concentration.

The effects of the interaction between current and cathode age (X_1X_2), and that between CO_2 concentration and cathode age (X_2X_3) were statistically insignificant. Nevertheless the weak effect of the interaction between the CO_2 concentration and cathode age suggests that the cathode deactivation rate was decreased by a lower CO_2 concentration and/or that the primary cathode reaction approached mass transfer control when the CO_2 feed concentration dropped to 33 vol%.

4.2. *Parametric experiments*

4.2.1 *Current*

Figure 4 shows the effect of current on the formate current efficiency with fixed cathode age (10 min) and CO_2 feed concentration (100 vol%). The CE values increased monotonically with decreasing current, reaching

Table 4. Current efficiencies and carbon balance for 16 runs of the factorial set

Run	E_{cell} (V)	CE%					Total CE (%)	Carbon balance closure (%)
		$HCOO^-$	H_2	CO	CH_4	C_2H_4		
1–16	3.9–5.9	23–71	24–86	0.0–5	0.0–0.3	0.0	95–134*	97–106
					Mean (std. dev.)		105(10)	101(3)

CE = current efficiency.
*A high "Total CE" in two runs is suspected to be the result of errors in the Orsat analysis at high CO_2 levels (>80 vol%) which lead to an overestimate of the hydrogen content of the product gas.
The formate CE is not affected by this Orsat error.

Table 5. Summary of the calculated factorial effects

Effects	Main			Interaction			95% confidence intervals	Curvature	95% confidence intervals
	Current X_1	Cathode age X_2	$y_{CO_2}X_3$	X_1X_2	X_2X_3	X_1X_3			
$HCOO^-$ CE%	−24.4	−6.9	14.6	0.9	−2.2	8.2	±3.1	0.7	±2.8
[$HCOO^-$] mM	14.7	−2.7	11.6	0.8	−2.1	9.8	±3.8	−3.3	±3.6

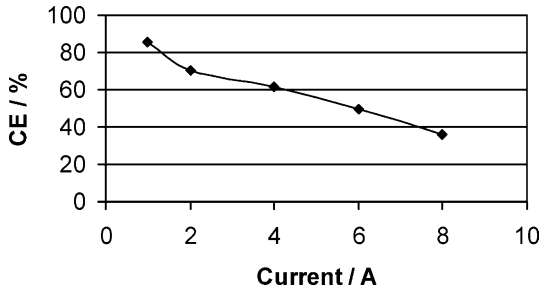

Fig. 4. Effect of current on formate CE. yCO_2: 100 vol%; cathode age: 10 min.

86% at 1 A, which corresponds to a superficial current density of 0.22 kA m^{-2} (22 mA cm^{-2}). The $HCOO^-$ concentration reached the maximum of 45 mM at 6 A (1.33 kA m^{-2}), where the CE was 50%, and corresponded to a partial current density for CO_2 reduction to formate of 0.67 kA m^{-2} with a reactor voltage of 5.80 Volt and specific energy of 621 kWh $kmol^{-1}$ of formate.

Table 6 lists the literature data on tin electrodes and some experimental data from the present work. These data show the benefit of using a 3D cathode with co-current G/L flow in a continuous reactor to drive the process at a useful current density.

4.2.2. *CO_2 feed concentration*

Figure 5 shows the effect of CO_2 feed concentration in the gas phase on the formate CE under fixed current (6 A) and cathode age (10 min). Here the CE increased monotonically with CO_2 concentration (i.e. CO_2 partial pressure), as expected in this process where CO_2(aq) was the primary electro-active species.

4.2.3. *Operating time*

Deactivation of the cathode was observed during the factorial runs, and more experiments were conducted to investigate this effect. Figure 6 shows the "deactivation" patterns under different operating conditions, while Figure 7 and Table 7 present results of SEM and EDX measurements on the new and used cathodes.

Figures 7a(i) and (ii) show the new tinned-copper mesh at 1 mm and 5 μm magnification, respectively, while Figures 7b(i) and (ii) show the corresponding photographs of the used tinned-copper mesh with 100 min of operating time. The SEM images show that the number of white spots, which are copper, increases with time. This observation matches the EDX analyses in Table 7, which show the Sn/Cu ratio on the surface dropping with time, at a rate that apparently increased with the CO_2 concentration in the feed gas. Tin is being lost and copper is being exposed on the cathode surface while the reactor is in operation. The reason for this loss of tin is not clear but it is almost certainly the cause of the "deactivation" of the cathode with respect to formate generation, since the hydrogen over-potential of copper is about 0.3 V less negative than that of tin.

In Figure 6 the current efficiency for formate at 6 A drops more sharply with time under 100 vol% CO_2 than under 33 vol% CO_2. This effect of CO_2 concentration and time is reflected in the factorial data of Figure 3 and may be due to an increase in the rate of cathode deactivation with CO_2 pressure and/or to the fact that at 33 vol% CO_2 the primary reaction is under (or close to) mass transfer control and thus relatively insensitive to the conditions of the cathode surface that dictate the intrinsic reaction kinetics. The latter reason is supported by the model described in the Appendix, that estimates the CO_2 mass transfer limited current with 33 vol% CO_2 as about 1.6 A.

5. Overall (full-cell) reactions and performance indicators

For a practical process development, it is necessary to examine the reactions, material balance and performance indicators (i.e. figures of merit) for the overall reactor. Considering only the production of formate and its competing reaction of hydrogen evolution at the cathode, plus the oxygen evolution at the anode, the full-cell reactions A and B are obtained by combining the respective cathode and anode half-cell reactions (with potassium as the principal cation) and adding the subsequent reaction of CO_2 with hydroxide in the bulk catholyte. The cation membrane separator prevents the transport of hydroxide from the cathode to the anode.

Table 6. Comparison of the present work with literature data on tin electrodes[a]

Authors	Electrolyte	Temperature (K)	CD (kA m^{-2})	CE for $HCOO^-$ (%)
This work	0.45 M $KHCO_3$	ca. 298	0.22	86
	0.45 M $KHCO_3$	ca. 298	1.78	36
Y. Hori [4]	0.5 M $KHCO_3$	Ambient	0.06	66 ~ 80
F. Koleli [7]	0.5 M $KHCO_3$	Ambient	0.04	20
S. Ikeda [20]	0.1 M TEAP[b]	Ambient	NA	68
M. Azuma [21]	0.05 M $KHCO_3$	273	NA	29

CD = superficial current density.
CE = current efficiency.
[a]All the data were obtained under ambient pressure.
[b]TEAP: tetraethyl ammonium perchlorate.

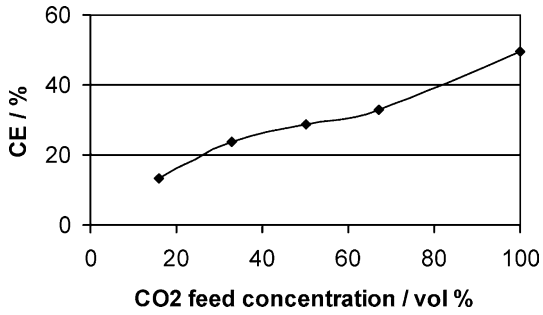

Fig. 5. Effect of CO_2 concentration on formate CE. Current: 6 A; cathode age: 10 min.

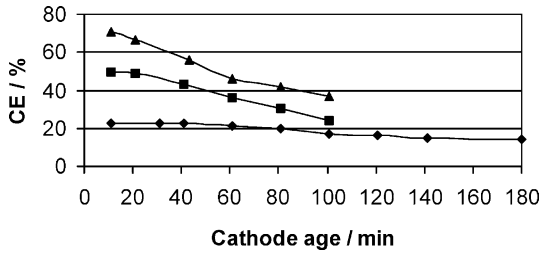

Fig. 6. Effects of cathode age on formate CE. ▲2 A and 100% CO_2 gas feed; ■6 A and 100% CO_2 gas feed; ◆6 A and 33% CO_2 gas feed.

Cathode	[1]	$CO_2(aq) + H_2O + 2e^- \rightarrow HCOO^- + OH^-$
Cathode	[2]	$2H_2O + 2e^- \rightarrow H_2 + 2OH^-$
Anode	[3]	$2OH^- \rightarrow 1/2O_2 + H_2O + 2e^-$
Bulk catholyte	[4]	$CO_2 + OH^- \rightarrow HCO_3^-$
Full-cell	[A]	$2KOH + 2CO_2 \rightarrow HCOOK + KHCO_3 + 1/2O_2$ (2 Faraday)
Full-cell	[B]	$2KOH + 2CO_2 + H_2O \rightarrow 2KHCO_3 + H_2 + 1/2O_2$ (2 Faraday)

The overall carbon (material) balance was checked for each factorial run in terms of the carbon closure, which is defined as:

$$\text{Carbon closure} = [\text{Carbon out}/\text{Carbon in}] \times 100\%$$

The data in Table 4 give an average (steady-state) carbon closure of 101% with a standard deviation of 3%. By the Students' *t*-test (95% confidence level), the average carbon closure is not statistically different from 100% [19], so it appears the analyses give an adequate account of the reaction products. The total CE's in Table 4 were calculated by summing the CE's for all the measured products. Anomalously high total CE's for two runs were probably caused by the errors in the Orsat analysis for CO_2, which is problematic for CO_2 concentrations over about 80 vol%.

The consumption of CO_2 is that from both reactions A and B, which amounts to 1 mol CO_2 per Faraday.

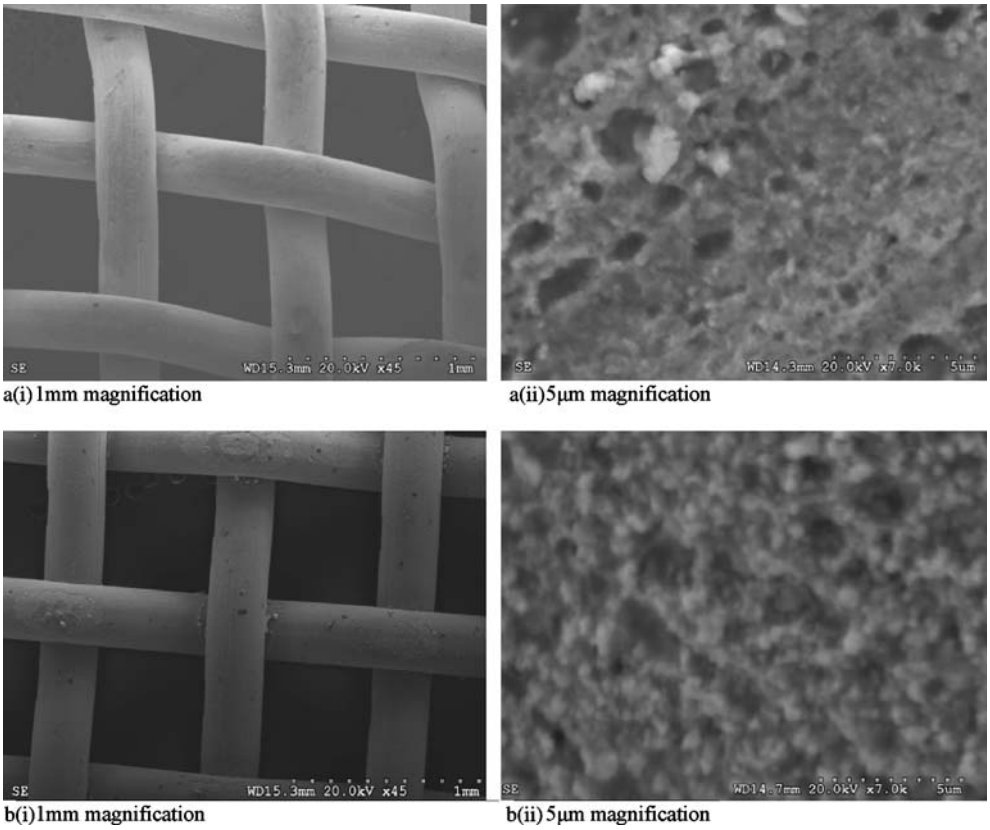

Fig. 7. SEM images of tinned-copper mesh cathodes: a(i) and (ii) new. b(i) and (ii) with 100 min operating time. *Note*: a(i) and b(i): 1 mm magnification; a(ii) and b(ii): 5 μm magnification.

Table 7. EDX analyses for tinned copper cathode mesh

Mesh description	Catalytic activity	Sn/Cu ratio on the surface
New	Highest	1/1.05
30 min under 33% CO_2 at 6 A	High	1/1.74
30 min under 100% CO_2 at 6 A	Middle	1/2.10
100 min under 100% CO_2 at 6 A	Low	1/5.10

Thus the conversion of CO_2 and yield of formate from CO_2 are given respectively by:

$$\text{Conversion of } CO_2 = x = (I/F)/(CO_2 \text{ feedrate})$$

[CO_2 dissolved in the electrolyte is assumed unconverted]

$$\text{Yield of } HCOO^- \text{ from } CO_2 = (CE_A/2)x$$

The specific energy, space-time yield for formate and mean residence time of catholyte in the reactor are calculated from:

$$SE = 2F(E_{cell})/(3600CE_A)$$

$$STY = CE_A I/(2F(\text{cell volume}))$$

$$\text{Residence time} \approx (\text{cathode volume})(\text{porosity})/[\text{volumetric (gas + liquid) flow}]$$

(assumes zero G/L slippage)

Values of these performance indicators are summarized in Table 8 and imply that there is potential for development of the electro-reduction of CO_2 to a practical process for the production of formates or formic acid. However, with formic acid priced about 1 \$US kg^{-1} and carbon credits around 10 \$US ton^{-1} CO_2 such a process would not now be economically viable.

6. Reactor model

The main results of this work can be interpreted in terms of the crude model of the cathode processes detailed in the Appendix. In this model, the system is simplified by taking the primary and secondary cathode reactions as respectively the reduction of CO_2 to formate and the reduction of water to hydrogen, with the assumption of uniform current density over the cathode surface. The *intrinsic* kinetics of both reactions is assumed to take the Tafel form (i.e. the high-field approximation to the Butler–Volmer equation), with the primary reaction under a mass transfer constraint that does not allow its partial current density to exceed the CO_2 mass transfer limited value (i.e. so called "mixed control"). These assumptions give the set of simultaneous (non-linear) equations that is elaborated in the Appendix and embodied in an Excel spreadsheet. The spreadsheet (not included here) uses about 100 lines of code in the iterative mode to calculate the factors that contribute to the model (e.g. CO_2(aq) concentration, equilibrium potentials, Reynolds' numbers, mass transfer coefficient, tin coverage, etc.) and to solve the equations.

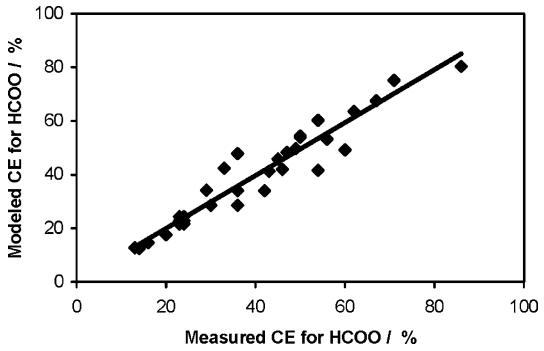

Fig. 8. Correlation of measured versus modeled results.

For a specified total current the cathode overpotential equations are solved for the partial current density (CD) of each reaction to give the modeled current efficiency (CE) for $HCOO^-$ (i.e. the formate CE) as:

$$\text{Modeled CE for } HCOO^- = \text{Formate CE} = \text{primary CD/total CD}$$

Figure 8 shows the correlation between the 33 values of formate CE that were measured in the experiments and calculated by this model. The model contains three adjustable parameters, specifically the Tafel constant for the primary reaction (set at −0.40 V) and the two

Table 8. Performance indicators measured in bench-scale experiments

Performance indicator	Units	Range
Current density (superficial)	kA m^{-2}	0.22–1.78
Reactor voltage	Volt per cell	3–6
Current efficiency for $HCOO^-$	%	86–13
Specific energy for $HCOO^-$	kWh $kmol^{-1}$	300–1300
Conversion of CO_2	%	20–80
Yield of organics from CO_2	%	6–17
Space-time-yield of $HCOO^-$	kmol m^{-3} s^{-1}	$(2–6) \times 10^{-4}$
Product concentration of $HCOO^-$	kmol m^{-3}	$(5–47) \times 10^{-3}$
Catholyte residence time	s	ca. 5
Product gas H_2 concentration	vol%	20–80

constants fitted to capture the effect of operating time on the tin coverage of the cathode surface in the expression: $\theta = 0.66[\exp(-0.015t)]$.

7. Conclusions

The electro-reduction of carbon dioxide to formate can be carried out in a continuous reactor with co-current flow of carbon dioxide gas and an aqueous catholyte solution through a fixed-bed cathode. This principle has been tested by experiments in a laboratory bench-scale membrane reactor with a cathode consisting of a single 0.150 m by 0.030 m layer of $30^{\#}$ mesh tinned-copper, using gas (CO_2 + N_2) and liquid (0.45 M $KHCO_3$) flows of respectively 180 ml min^{-1} STP and 20 ml min^{-1} near ambient conditions with currents from 1 to 8 A.

The experimental results indicate that the primary and secondary products are respectively formate and hydrogen, with tertiary products including CO, CH_4, C_2H_4 and possibly $HCHO/CH_3OH$. Factorial and parametric data, backed by a crude model of the cathode process, support CO_2(aq) as the initial electro-active species in a primary reaction subject to CO_2 mass transfer constraint, with current efficiency depending on the current density and partial pressure of CO_2 in the gas phase, together with the hydrogen over-potential and mass transfer capacity of the 3D cathode. Under a CO_2 pressure of 115 kPa(abs) at 300 K in 0.47 M $KHCO_3$, the mass transfer limited superficial current density is estimated as about 1 kA m^{-2} and in corresponding experiments on a "fresh" tinned cathode formate is generated at superficial partial current density up to about 0.7 kA m^{-2}. The current efficiency for formate decreases with time due to the progressive loss of tin from the cathode surface to expose the copper substrate, with a consequent increase in the exchange current density for hydrogen evolution that promotes the electro-reduction of water relative to that of carbon dioxide.

The overall cell process consumes hydroxide from the anolyte and results in the transfer of CO_2 into the catholyte to give formate, together with bicarbonate to match the hydroxyl generation in the cathode reactions. The material balance for the process thus involves transport of cations (e.g. K^+) across the membrane to match the total conversion of CO_2, while a fraction of these cations (equivalent to the formate yield) goes to the formate salt. As well as the bicarbonate, major side products of this process are stoichiometric oxygen and substantial amounts of hydrogen.

The performance indicators calculated from the experimental results and summarized in Table 8 imply that if the rapid deterioration of the cathode can be prevented the electro-reduction of CO_2 to formate has potential for development to a practical (albeit expensive) process.

Acknowledgements

This work was funded by the Natural Sciences and Engineering Research Council of Canada (NSERC) and supported by the University of British Columbia.

Appendix: Reactor (cathode) modeling

All symbols used here are defined in the Nomenclature.

This crude model of the cathode processes is based on isothermal operation of an open system at steady-state, with the following two reactions at the cathode:

		$E^oVSHE@298K$
[1]	$CO_2(aq)+H_2O+2e^- \rightarrow HCOO^- + OH^-$	−1.02
[2]	$2H_2O+2e^- \rightarrow H_2+2OH^-$	−0.83

The equilibrium potential of each reaction comes from the Nernst equation:

$$E_{r,1} = E_1^o + (RT/2F)\ln\{(p_{CO_2}/101)/[HCOO^-][OH^-]\}$$
$$E_{r,2} = E_2^o + (RT/2F)\ln\{(101/p_{H_2})[OH^-]^2\}$$

The primary reactant (CO_2(aq)) reaches the cathode by absorption of CO_2 from the gas phase into the flowing catholyte and mass transfer of CO_2(aq) to the liquid/solid (L–S) interface. Assuming gas–liquid (G–L) equilibrium, the bulk concentration of CO_2(aq) in the catholyte is determined by:

$CO_2(g) \leftrightarrow CO_2(aq)$	absorption
$CO_2(aq) + H_2O(l) \leftrightarrow H_2CO_3$	hydrolysis

These reactions are combined to give the pseudo-equilibrium:

$$CO_2(g) + H_2O(l) \leftrightarrow H_2CO_3^* \quad \text{for which:}$$

$$K_o = [H_2CO_3^*]/p_{CO_2} = 2.94 \times 10^{-4} \text{ at } 298 \text{ K} \quad [22]$$

where $[H_2CO_3^*] \equiv [CO_2(aq)] + [H_2CO_3]$

The concentration of CO_2(aq) in this system is calculated from the equilibrium:

$$K' = [H_2CO_3]/[CO_2(aq)] \approx 2.6 \times 10^{-3} \text{ at } 298 \text{ K} \quad [23]$$

i.e. at equilibrium ca. 99.7% of the dissolved CO_2 is present as CO_2(aq), while 0.3% is carbonic acid (H_2CO_3).

The H_2CO_3 in solution subsequently dissociates according to the pseudo-equilibrium:

$$H_2CO_3^* \leftrightarrow H^+ + HCO_3^-$$

Table A.1. Modeling values

Input values			Calculated values		
Variable	Units	Value	Variable	Units	Value (range)
a	m^{-1}	7740	$[CO_2(aq)]$	kmol m^{-3}	$(0.54–3.36) \times 10^{-2}$
a_1	V	−0.40	CE_1	%	18–81
a_{2Sn}	V	−0.90	E	V(SHE)	−1.1 to −1.3
a_{2Cu}	V	−0.60	E_{r1}	V(SHE)	−0.77 to −0.81
D	$m^2\ s^{-1}$	1.84×10^{-9}	E_{r2}	V(SHE)	−0.44 to −0.47
d	m	0.305×10^{-3}	h	–	0.78
d_b	m	50×10^{-6}	i_{1L}	kA m^{-2}	0.17–1.06
ΔE	V	0.5	j_{1L}	kA m^{-2}	0.037–0.218
G	kg $m^{-2}\ s^{-1}$	0.294	K_o	M kPa^{-1}	2.94×10^{-4}
$[HCO_3^-]$	kmol m^{-3}	0.47	K_1	M	4.53×10^{-7}
i	kA m^{-2}	0.22–1.78	k_F	m s^{-1}	2.32×10^{-5}
L	kg $m^{-2}\ s^{-1}$	18.2	k_G	m s^{-1}	$(0.52–2.7) \times 10^{-5}$
P	kPa(abs)	115	k_M	m s^{-1}	$(2.4–3.6) \times 10^{-5}$
pCO_2	kPa(abs)	18–115	k_{Ma}	s^{-1}	0.18–0.28
T	K	298	pH	–	7.2–8.0
t	min	10–180	SE	kWh $kmol^{-1}$	300–1300
ε	–	0.41			
κ	S m^{-1}	3.86	κ_e	S m^{-1}	0.92
γ	–	0.7			
μ_g	kg $m^{-1}s^{-1}$	1.6×10^{-5}	η_1	V	−0.38 to −0.51
μ_l	kg $m^{-1}s^{-1}$	9.5×10^{-4}	η_2	V	−0.70 to −0.83
ρ_g	kg m^{-3}	1.79	θ	–	0.1–0.6
ρ_l	kg m^{-3}	1030			
τ	m	0.61×10^{-3}	τ_{eff}	m	$(0.7–1.8) \times 10^{-3}$

$$K_1 = (\gamma^2)[H^+][HCO_3^-]/[H_2CO_3^*] = 4.53 \times 10^{-7} \text{ at } 298\,K \quad [24]$$

$$\text{For } 0.47\,m\,KHCO_3 \text{ at } 298\,K: \quad \gamma \approx 0.7 \quad [25]$$

The bulk concentration of CO_2(aq) and the catholyte pH are obtained by solving the above equations, using the average values of $[HCO_3^-]$ and p_{CO_2} over the reactor at 298 K.

Assuming the intrinsic kinetics of both reactions fit the Tafel form, with reaction 1 under a CO_2 mass transfer constraint, the individual over-potentials (η_1 and η_2) are related to the partial current densities (j_1 and j_2) by:

$$\eta_1 = E - E_{r,1} = a_1 - 0.12\log(j_1) + 0.12\log(1 - j_1/j_{1L}) \quad \text{On tin and on copper}$$
$$\eta_2 = E - E_{r,2} = a_{2Sn} - 0.12\log(j_2) \quad \text{On tin}$$
$$\eta_2 = E - E_{r,2} = a_{2Cu} - 0.12\log(j_2) \quad \text{On copper}$$

The CO_2 mass transfer limited current density (j_{1L}) is found from the bulk concentration of CO_2(aq) and the liquid to solid (L–S) mass transfer coefficient (k_M) for CO_2(aq) to the 3D cathode surface. For this purpose, the value of k_M is estimated as that due to forced convection in 2-phase flow (k_F), enhanced by a factor (k_G) from the cogeneration of hydrogen gas, whose partial current density (j_2) gives the Reynolds' number (Re_b) for gas bubble evolution at the cathode surface:

$$k_F = (D/d)(2.85Sc^{0.33}\ Re_l^{0.125}\ Re_g^{0.238}) \quad [26]$$

$$k_G = (D/d_b)(0.93Re_b^{0.5}Sc^{0.487}) \quad [27]$$

$$Re_b = (2Fj_2RT/P)(d_b\rho_l/\mu_l)$$

$$k_M = k_F[1 + (k_G/k_F)^2]^{0.5}$$

Then:

$$j_{1L} = 2Fk_M[CO_2(aq)]$$

To check the electro-active thickness of the 3D cathode, the liquid hold-up (h) and corresponding effective conductivity of the catholyte (κ_e) are calculated from:

$$h = 1 - 0.907[L^{-0.362}G^{0.301}] \quad [15]$$

$$\kappa_e = 2\kappa h\varepsilon/(3 - h\varepsilon)$$

Then the effective electro-active thickness under pure mass transfer control (τ_{eff}) is estimated by:

$$\tau_{eff} = 2\kappa_e(\Delta E)/(2Fk_M a[CO_2(aq)])$$

with the potential window (ΔE) set at 0.5 Volt. Assuming uniform current density on the cathode surface, the over-potential equations are solved for the partial current densities to give the current efficiency for reaction 1:

$$CE_1 = j_1/(j_1 + j_2)$$

The decreasing tin content of the cathode surface is accounted for by assigning a tin coverage (θ) and approximating the Tafel constant for reaction 2 as the linear combination:

$$a_2 = a_{2Cu} + \theta(a_{2Sn} - a_{2Cu})$$

Values of θ calculated to fit the data for all 33 experimental runs range from about 0.6 to 0.1 and are correlated by:

$$\theta = 0.66\exp(-0.015t)$$

The CO_2 conversion is estimated by integrating the partial current densities over the cathode surface and assuming that all hydroxide from reactions 1 and 2 combines with CO_2 to form bicarbonate, i.e.

$$CO_2 + OH^- \rightarrow HCO_3^-$$

Potassium cations (K^+) transfer across the membrane to match the total current and give potassium formate ($KHCO_2$) and potassium bicarbonate ($KHCO_3$), together with hydrogen (H_2), as the net cathode products.The model involves the set of simultaneous non-linear equations outlined above, embodied in an Excel spreadsheet that runs in the iterative mode to calculate CE_1, which is the equivalent of the experimentally measured formate CE and of CE_A introduced in Section 6. When the coverage correlation is used in the model along with the input parameters listed in Table A.1 the agreement between the measured and modeled current efficiency for formate is that shown in Figure 8. The values in Figure 8 are correlated by a straight line with a slope of 0.99, an intercept of 0.3% and regression coefficient of 0.96.Ranges of some important input and calculated values in this model are summarized in Table A.1.

References

1. M. Ladouceur and G. Bélanger, *Can. Chem. News*. **6** (2001) 17.
2. R.P.S. Chaplin and A.A. Wragg, *J. Appl. Electrochem.* **33** (2003) 1107.
3. M. Jitaru, D.A. Lowy, M. Toma, B.C. Toma and L. Oniciu, *J. Appl. Electrochem.* **27** (1997) 875.
4. Y. Hori, K. Kikuchi and S. Suzuki, *Chem. Lett*. (1985) 1695.
5. K. Hara, A. Kudo and T. Sakata, *J. Electroanal. Chem.* **391** (1995) 141.
6. T. Mizuno, K. Ohta and A. Sasaki, *Energy Sources* **17** (1995) 503.
7. F. Köleli, T. Atilan and N. Palamut, *J. Appl. Electrochem.* **33** (2003) 447.
8. S. Kapusta and N. Hackerman, *J. Electrochem. Soc*. **130**(3) (1983) 607.
9. Y.B. Vassiliev and V.S. Bagotzky, *J. Electroanal. Chem*. **189** (1985) 271.
10. K.S. Udupa, G.S. Subramanian and H.V.K. Udupa, *Electrochim. Acta*. **16** (1971) 1593.
11. K. Hara and T. Skata, *J. Electrochem. Soc*. **144** (1997) 539.
12. H. Yano, F. Shirai, M. Nakayama and K. Ogura, *J. Electroanal. Chem*. **519** (2002) 93.
13. Y. Akahori, N. Iwanaga, Y. Kato, O. Hamamoto and M. Ishii, *Electrochemistry (Tokyo, Japan)* **72**(4) (2004) 266.
14. C. Oloman, *J.Electrochem. Soc*. **126**(11) (1979) 1885.
15. I. Hodgson and C. Oloman, *Chem. Eng. Sci*. **54** (1999) 5777.
16. http://www.finishing.com/0200–0399/260.html.
17. A.I. Vogel, 'A Text Book of Quantitative Inorganic Analysis' (Longmans, New York, 1978).
18. C. Oloman, 'Reactor Design in Electro-Organic Synthesis', Tutorial Lectures in Electrochemical Engineering. A.I.Ch.E. Symposium Series **229**(79) (1984) 68.
19. T.D. Murphy, *Chem. Eng*. **6** (1977) 168.
20. S. Ikeda, T. Takagi and K. Ito, *Bull. Chem. Soc. Jpn*. **60** (1987) 2517.
21. M. Azuma, K. Hashimoto, M. Hirmoto, M. Watanabe and T. Sakata, *J. Electrochem. Soc*. **137** (1990) 1772.
22. R.H. Perry and C.H. Chilton (ed.), *Chemical Engineers' Handbook*, 5th ed., (McGraw Hill, New York, 1973).
23. F.R. Keene, *Electrochemical and Electro-catalytic Reactions of Carbon Dioxide* (Elsevier, Amsterdam, 1993).
24. L. Benefield, J. Judkins and B. Weand, *Process Chemistry for Water and Wastewater Treatment* (Prentice-Hall, Inglewood Cliffs, 1982).
25. A.C. Walker, U.B. Bray and K. Johnston, *J. Am. Chem. Soc*. **49** (1927) 1235.
26. L. Coppola, O. Cavatort and U. Bohm, *J. Appl. Electrochem*. **19** (1989) 100.
27. K. Stephan and H. Vogt, *Electrochim. Acta* **24** (1979) 11.